

Two-loop electroweak corrections for the $K \rightarrow \pi\nu\bar{\nu}$ decays

Joachim Brod,¹ Martin Gorbahn,^{1,2} and Emmanuel Stamou^{1,2,3}

¹*Excellence Cluster Universe, Technische Universität München, Boltzmannstraße 2, D-85748 Garching, Germany*

²*Institute for Advanced Study, Technische Universität München, Lichtenbergstraße 2a, D-85748 Garching, Germany*

³*Physik-Department, Technische Universität München, James-Frank-Straße, D-85748 Garching, Germany*

(Received 8 November 2010; published 22 February 2011)

The rare $K \rightarrow \pi\nu\bar{\nu}$ decays play a central role in testing the standard model and its extensions. Upcoming experiments plan to measure the decay rates with high accuracy. Yet, unknown higher-order electroweak corrections result in a sizeable theory error. We remove this uncertainty by computing the full two-loop electroweak corrections to the top-quark contribution X_t to the rare decays $K_L \rightarrow \pi^0\nu\bar{\nu}$, $K^+ \rightarrow \pi^+\nu\bar{\nu}$, and $B \rightarrow X_{d,s}\nu\bar{\nu}$ in the standard model. The remaining theoretical uncertainty related to electroweak effects is now far below 1%. Finally we update the branching ratios to find $\text{Br}(K_L \rightarrow \pi^0\nu\bar{\nu}) = 2.43(39)(6) \times 10^{-11}$ and $\text{Br}(K^+ \rightarrow \pi^+\nu\bar{\nu}) = 7.81(75)(29) \times 10^{-11}$. The first error summarizes the parametric, the second the remaining theoretical uncertainties.

DOI: 10.1103/PhysRevD.83.034030

PACS numbers: 13.25.Es, 12.15.Hh, 12.15.Lk

I. INTRODUCTION

The branching ratios of the rare $K^+ \rightarrow \pi^+\nu\bar{\nu}$ and $K_L \rightarrow \pi^0\nu\bar{\nu}$ decays are dominated by contributions of internal top quarks in the standard model. This short-distance sensitivity results in a precise theory prediction, but also in a proportionality to powers of $V_{ts}^*V_{td}$. Accordingly, the branching ratios are suppressed with respect to generic new physics scenarios by the near diagonality of the Cabibbo-Kobayashi-Maskawa (CKM) matrix. This leads to a high sensitivity to new physics, and a precision measurement of these modes could provide a decisive test of the standard model and its extensions.

This potential will be exploited by a new generation of experiments (NA62 at CERN, KOTO at JPARC, and the proposed future experiment P996 at Fermilab), which aim at measuring the branching ratios with unprecedented precision.

In the standard model the $K \rightarrow \pi\nu\bar{\nu}$ decays proceed through Z penguin and electroweak box diagrams which exhibit a powerlike Glashow-Iliopoulos-Maiani mechanism. This implies a suppression of nonperturbative effects and, related to this, that the low-energy effective Hamiltonian [1,2]

$$\mathcal{H}_{\text{eff}} = \frac{4G_F}{\sqrt{2}} \frac{\alpha}{2\pi\sin^2\theta_W} \sum_{l=e,\mu,\tau} (\lambda_c X^l + \lambda_t X_t) (\bar{s}_L \gamma_\mu d_L) \times (\bar{\nu}_{lL} \gamma^\mu \nu_{lL}) + \text{H.c.} \quad (1.1)$$

involves to an excellent approximation only a single effective operator. Here G_F is the Fermi constant, α the electromagnetic coupling and θ_W the weak mixing angle. The sum is over all lepton flavors, $\lambda_i = V_{is}^*V_{id}$ comprise the CKM factors, and f_L represents left-handed fermion fields.

The functions X^l constitute the charm-quark contribution to \mathcal{H}_{eff} and add 30% to the total branching ratio of the $K^+ \rightarrow \pi^+\nu\bar{\nu}$ decay, while they leave the CP -violating $K_L \rightarrow \pi^0\nu\bar{\nu}$ decay unaffected. The theoretical uncertainty

in X^l is 2.5% after next-to-next-to-leading order QCD [3–5] and next-to-leading order (NLO) electroweak corrections [6] are taken into account, and the resulting error in the branching ratio is small.

The situation is different for the function X_t which includes internal top-quark loops: it gives either the sole or the dominant contribution to the neutral or the charged decay modes, respectively. A two-loop electroweak calculation should cancel the sizeable scheme dependence of the input parameters. Yet, only NLO QCD corrections [2,7,8] and the leading term of the large- m_t expansion of the two-loop electroweak corrections are known. While unknown higher-order QCD corrections result in a 1% uncertainty in X_t , the uncertainty related to unknown subleading electroweak contributions is estimated to be $\pm 2\%$ [9]. This can be understood in the following way: the matching calculation with internal top-quark loops is purely short distance, the resulting operator renormalizes like a current, such that the QCD perturbation theory converges well. Yet the on-shell scheme counterterm of $\sin\theta_W$ includes large higher terms in the large- m_t expansion. Hence the renormalization scheme dependence of $\alpha/\sin^2\theta_W$ in (1.1) cannot cancel if only the leading term in the large- m_t expansion is taken into account. This was found in Ref. [9] where the scheme difference between the on-shell scheme and the $\overline{\text{MS}}$ scheme was only decreased from 5.6% to 3.4% through the inclusion of the first order in the large- m_t expansion.

In this paper we will improve on the analysis of Ref. [9] and compute the full electroweak two-loop corrections to the top-quark contribution X_t . Only in such a way is it possible to fix the definition of the electroweak input parameters and reduce the uncertainty due to unknown higher-order electroweak corrections from 2% to the per mil level. Since a 2% uncertainty in X_t scales up to a 3% to 4% uncertainty in the branching ratios such a reduction of the theoretical error is important, in particular, in light of

the coming experiments. In addition, our results are equally applicable for the $B \rightarrow X_{d,s} \nu \bar{\nu}$ decays.

Our paper is organized as follows. In Sec. II we discuss the dependence of our result on different renormalization schemes. In Sec. III we present some technical details of our calculation. Our numerical results are contained in Sec. IV. In the Appendices we provide the analytic form of the electroweak correction to X_t in the limit of small $\sin\theta_W$ and compare our expansion for a large top-quark mass with the literature.

II. X_t BEYOND LEADING ORDER

The truncation of the perturbation theory results in a residual scale and scheme dependence of the matrix elements of the effective Hamiltonian in Eq. (1.1). For the top-quark contribution, the matrix element of the operator

$$Q_\nu = \sum_{l=e,\mu,\tau} (\bar{s}_L \gamma_\mu d_L) (\bar{\nu}_{lL} \gamma^\mu \nu_{lL}) \quad (2.1)$$

factorizes and $4\alpha G_F / (2\sqrt{2}\pi \sin^2\theta_W) \lambda_t X_t$ will be independent of the renormalization procedure after higher-order corrections are included. Let us now discuss the dependence on the electroweak renormalization scheme and how to combine these schemes with the NLO QCD results, which are known in the $\overline{\text{MS}}$ scheme.

Pure QCD corrections leave G_F , α , and $\sin^2\theta_W$ unaffected, such that X_t is a renormalization scheme invariant quantity if electroweak effects are ignored. It is then customary to expand

$$X_t = X_t^{(0)} + \frac{\alpha_s}{4\pi} X_t^{(1)} + \frac{\alpha}{4\pi} X_t^{(EW)} \quad (2.2)$$

in terms of the leading-order (LO) contribution [10]

$$X_t^{(0)} = \frac{x_t}{8} \left[\frac{x_t + 2}{x_t - 1} + \frac{3x_t - 6}{(x_t - 1)^2} \ln x_t \right], \quad (2.3)$$

where $x_t = m_t^2/M_W^2$. The schemes for m_t and M_W are defined below. The NLO QCD correction [2,7,8]

$$\begin{aligned} X_t^{(1)} = & -\frac{29x_t - x_t^2 - 4x_t^3}{3(1-x_t)^2} - \frac{x_t + 9x_t^2 - x_t^3 - x_t^4}{(1-x_t)^3} \ln x_t \\ & + \frac{8x_t + 4x_t^2 + x_t^3 - x_t^4}{2(1-x_t)^3} \ln^2 x_t - \frac{4x_t - x_t^3}{(1-x_t)^2} \text{Li}_2(1-x_t) \\ & + 8x_t \frac{\partial X_t^{(0)}}{\partial x_t} \ln \frac{\mu_t^2}{M_W^2} \end{aligned} \quad (2.4)$$

fixes the renormalization scheme of the parameters which appear in the LO contribution: namely, the top-quark mass. Here, the QCD part of the top-quark mass counterterm is defined in the $\overline{\text{MS}}$ scheme.

The leading term in the large- m_t expansion of the two-loop electroweak corrections $X_t^{(EW)}$ can be found in Ref. [9], while the hitherto unknown full two-loop result is computed in this paper. The sum of $X_t^{(0)}$ and $X_t^{(EW)}$ will

only be invariant under an electroweak scheme change if it is multiplied by the normalization factor of the effective Hamiltonian, $4\alpha G_F / (2\sqrt{2}\pi \sin^2\theta_W)$. Accordingly, the electroweak renormalization scheme has to be fixed for the parameters in the normalization factor.

Since in the electroweak theory not all parameters are independent, we have to specify the physical input parameters, and we choose the set

$$G_F, \alpha, M_Z, M_t, \quad \text{and} \quad M_H. \quad (2.5)$$

Here G_F is the experimental value of the Wilson coefficient relevant for muon decay, α the fine structure constant, and M_Z the Z -boson pole mass. M_t is the top-quark mass, where QCD corrections are renormalized in the $\overline{\text{MS}}$ scheme, while the on-shell scheme is used for the electroweak corrections. The Higgs mass M_H is essentially a free parameter—its value is assumed to be consistent with electroweak precision data.

For fixed input parameters we can now study the remaining residual higher-order uncertainty by using different renormalization schemes. In the following discussion we will make use of three renormalization schemes:

- (i) The $\overline{\text{MS}}$ scheme for all parameters,
- (ii) the on-shell scheme for all masses and the $\overline{\text{MS}}$ scheme for all coupling constants,
- (iii) or the on-shell scheme for all masses and the weak mixing angle—the QED coupling constant is renormalized in the $\overline{\text{MS}}$ scheme.

The explicit result for $X_t^{(EW)}$ is different for each renormalization scheme. In practice, we perform our calculation in the $\overline{\text{MS}}$ scheme and transform our result into the respective scheme by a finite renormalization.

In all three schemes we renormalize the CKM parameters in the $\overline{\text{MS}}$ scheme and use G_F as a normalization factor for the effective Hamiltonian in Eq. (1.1). The parameter G_F plays a special role, because it is by itself defined as a Wilson coefficient, of the operator $Q_\mu = (\bar{\nu}_{\mu L} \gamma_\rho \mu_L) \times (\bar{e}_L \gamma^\rho \nu_{eL})$ which induces the muon decay in the effective Fermi theory. To make this more explicit we introduce the following notation: We denote the Wilson coefficient for muon decay by $G_\mu = G_\mu^{(0)} + G_\mu^{(EW)} + \dots$, where the superscript (0) denotes the tree-level contribution, (EW) the one-loop electroweak corrections, and the ellipses stand for terms beyond second order in the electroweak interactions. By G_F we then denote the experimental value of G_μ as extracted from muon lifetime experiments [11,12]. If we now write the effective Hamiltonian (1.1) in the general form

$$\mathcal{H}_{\text{eff}} = \frac{4}{\sqrt{2}} \frac{\alpha}{2\pi \sin^2\theta_W} C_\nu Q_\nu = \frac{4G_F}{\sqrt{2}} \frac{\alpha}{2\pi \sin^2\theta_W} X_t Q_\nu, \quad (2.6)$$

we find

$$X_t^{(0)} = \frac{C^{(0)}}{G_\mu^{(0)}}, \quad X_t^{(EW)} = \frac{C^{(EW)}}{G_\mu^{(0)}} - \frac{C^{(0)}G_\mu^{(EW)}}{(G_\mu^{(0)})^2}. \quad (2.7)$$

A. The $\overline{\text{MS}}$ scheme

In the $\overline{\text{MS}}$ scheme we use

$$g_1, g_2, \nu, \lambda, \quad \text{and} \quad y_t \quad (2.8)$$

as fundamental parameters. Here g_1 and g_2 are the couplings of the $SU(2)$ and $U(1)$ gauge group, respectively, ν is the vacuum expectation value of the Higgs field, λ the quartic Higgs self-coupling, and y_t the Yukawa coupling of the top quark. All these parameters are running parameters, depending on the renormalization scale μ . We fix the initial conditions of these parameters by expressing the physical parameter set (2.5) through (2.8) using one-loop accuracy¹ and fitting the values of (2.8) to yield the experimental values of (2.5).

We choose to cancel all tadpole diagrams with a finite counterterm. This results in an additional finite renormalization of all massive quantities—a sample diagram is shown in Fig. 1. In this way we ensure that intermediate results are gauge parameter independent.

B. Masses in the on-shell scheme

As a more well-behaved alternative, we use the on-shell definition of the W -boson and the top-quark mass. Since we performed our calculation in the $\overline{\text{MS}}$ scheme, we have to perform a finite mass renormalization. The necessary renormalization constants consistent with our treatment of tadpole diagrams can be found in [13,14].

In addition, we have to specify the renormalization scheme for the weak mixing angle. We will use the following two schemes:

- (i) In the on-shell scheme the weak mixing angle is defined by $s_W^2 \equiv \sin^2 \theta_W^{\text{on-shell}} = 1 - M_W^2/M_Z^2$. Here the W -boson mass is calculated including radiative corrections from the input parameter set (2.5), which introduces a Higgs-mass dependence. In addition, the use of the on-shell value for $\sin^2 \theta_W$ implies a finite renormalization of our $\overline{\text{MS}}$ results by including a finite counterterm for $\sin^2 \theta_W$. It is given in terms of the on-shell renormalization constants for M_W and M_Z by

$$\delta s_W = \frac{c_W^2}{2s_W} \left(\frac{\delta M_Z^2}{M_Z^2} - \frac{\delta M_W^2}{M_W^2} \right) \Big|_{\Delta=0}, \quad (2.9)$$

where the subscript $\Delta = 0$ implies setting the pole part including the finite subtraction, $\Delta = 1/\epsilon - \gamma_E + \log 4\pi$, to zero. The expressions for δM_Z^2 and δM_W^2 can again be found in [13,14].

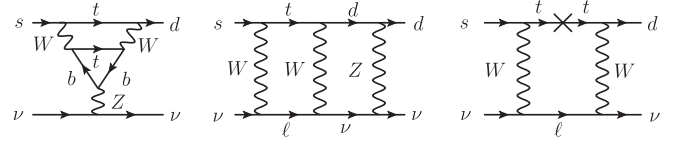


FIG. 1. Sample penguin, box, and counterterm diagrams. Our tadpole renormalization results in an explicit finite renormalization of all massive quantities. The right-hand side diagram shows a resulting counterterm diagram.

- (ii) The $\overline{\text{MS}}$ definition of the weak mixing angle, denoted by \hat{s}_{ND} , leads to numerically tiny NLO corrections. It is given in terms of s_W^2 by [15]

$$\hat{s}_{\text{ND}}^2 \equiv \sin^2 \theta_W^{\overline{\text{MS}}} = s_W^2 \left(1 + \frac{c_W^2}{s_W^2} \frac{4\pi \hat{\alpha}(M_Z)}{\hat{s}_{\text{ND}}^2} \Delta \hat{\rho} \right), \quad (2.10)$$

where $\hat{\alpha} = \alpha^{\overline{\text{MS}}}$, and $c_W^2 = 1 - s_W^2$. The explicit expression for $\Delta \hat{\rho}$ can also be found in [15].

The numerical discussion of the three different schemes is given in Sec. IV.

III. CALCULATION

We determine the effective Hamiltonian by computing the relevant standard model Green's functions in the $\overline{\text{MS}}$ scheme and matching them to the five-flavor effective theory. To this end we have to calculate two-loop box and penguin diagrams, samples of which are shown in Fig. 1. All diagrams reduce to two-loop vacuum diagrams after setting external momenta and light masses to zero. The resulting loop integrals are computed using standard methods [16,17]. All this is done in two independent setups: one is using the FEYNARTS [18] package to generate the diagrams and a self written MATHEMATICA program, the other method uses a self written FORM [19] program. The Feynman gauge $\xi = 1$ is used in both setups.

The integrals in the effective theory correspond to massless diagrams with vanishing external momenta and are exactly zero in dimensional regularization. The only remaining contributions are then products of renormalization constants and tree-level matrix elements of the operators Q_ν , defined in Eq. (2.1), and

$$E_\nu = \sum_{l=e,\mu,\tau} (\bar{s}_L \gamma_{\mu_1} \gamma_{\mu_2} \gamma_{\mu_3} d_L) (\bar{\nu}_{lL} \gamma^{\mu_1} \gamma^{\mu_2} \gamma^{\mu_3} \nu_{lL}) - (16 - 4\epsilon) Q_\nu. \quad (3.1)$$

The evanescent operator E_ν arises in the context of dimensional regularization and vanishes algebraically in four space-time dimensions. It leads to a nonvanishing finite contribution to the Wilson coefficient, proportional to the finite mixing of E_ν into Q_ν . The infinite operator renormalization constants are determined from the ultraviolet

¹For the Higgs-boson mass we use the tree-level relation.

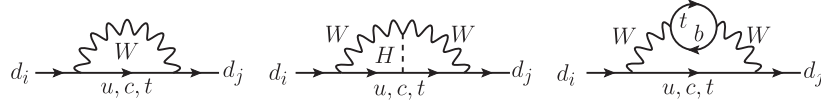


FIG. 2. Sample diagrams which imply an off-diagonal field renormalization.

poles of the matrix elements of the operators between external fermion states. They multiply the tree-level and one-loop Wilson coefficients of the operators (2.1) and (3.1) and cancel exactly the corresponding spurious infrared divergences of the standard model amplitude, thus rendering the matching condition finite.

The use of dimensional regularization is in general inconsistent with a fully anticommuting γ_5 matrix in d dimensions, and we use the 't Hooft-Veltman scheme in our calculation. However, problems only arise when computing traces containing at least three γ_5 matrices, appearing in the anomalous fermion triangles (see for instance the first diagram in Fig. 1). In all other cases we can use a naive anticommuting γ_5 (NDR scheme), which avoids spurious finite renormalizations required in the 't Hooft-Veltman scheme [20].

We have performed our calculation in the $\overline{\text{MS}}$ scheme as described in Sec. II. The renormalization of masses and couplings is performed in the usual way.

In order to ensure the canonical form of the kinetic term for the down-type quarks, $i\bar{d}_{L,k}\not{D}d_{L,j}$, in the effective theory, we perform a finite off-diagonal field renormalization. The exchange of W bosons induces transitions between quarks of different generations (cf. Figure 2). We re-diagonalize the kinetic term by including a suitable finite part in the (matrix-) field renormalization $Z_{L,ij}^{1/2}$:

$$d_{L,i}^{\text{bare}} = Z_{L,ij}^{1/2} d_{L,j}, \quad (3.2)$$

where i denotes the generation of the down-type fermion ($i = 1, 2, 3$).

The renormalization leads to a finite result for $X_i^{(EW)}$. As an additional check we also verified that the full result is analytically independent of the renormalization scale μ .

IV. NUMERICS

In this section we present our numerical results and discuss the theoretical uncertainty of the branching ratios of the rare Kaon decays. For our numerical analysis we use the central values and errors of the input parameters given in Table I. As discussed in detail in Sec. II, we use α , G_F , and M_Z as the basic input parameters for the electroweak theory. The mass of the W boson is then not an independent quantity; we calculate its mass using the approximate formula given in Ref. [27], which includes the state-of-the-art higher-order corrections.

Converting the on-shell top-quark mass M_t^{TEV} , measured at Tevatron, to the $\overline{\text{MS}}$ scheme using three-loop QCD accuracy, we find $M_t \equiv m_t^{\overline{\text{MS,QCD}}}(m_t) = 163.7$ GeV.

For this conversion as well as for the QCD running of M_t and α_s , we use the MATHEMATICA package RUNDEC [28].

The electroweak correction term $X_i^{(EW)}$ cancels the scheme and scale dependence of the prefactor $\alpha/\sin^2\theta_W$ up to higher orders in the electroweak interaction. The remaining scheme and scale dependence will serve as an estimate of the theoretical uncertainty of our result. To facilitate the discussion, we define the scale and scheme independent quantity

$$\tilde{X}_i = \frac{\alpha(\mu, M_H)}{\alpha(\mu = M_Z, M_H = 155 \text{ GeV})} \times \frac{\sin^2\theta_W(\mu = M_Z, M_H = 155 \text{ GeV})}{\sin^2\theta_W(\mu, M_H)} X_i(\mu). \quad (4.1)$$

It is formally independent of μ and coincides with $X_i(\mu)$ at $\mu = M_Z$ and $M_H = 155$ GeV. We normalize \tilde{X}_i to our central value for the Higgs-boson mass, $M_H = 155$ GeV; as we will see below, the dependence on M_H is very weak for $115 \text{ GeV} < M_H < 200 \text{ GeV}$. The function \tilde{X}_i is plotted in Fig. 3 for $M_H = 155$ GeV. Here the dashed line shows the LO result. As is clearly visible, the inclusion of the two-loop electroweak corrections (solid line) cancels the scale dependence of the electroweak input parameters almost completely, up to negligible corrections of 0.02%.

Next we discuss the dependence of our result on the choice of the renormalization scheme. The difference between the $\overline{\text{MS}}$ and on-shell definition of the parameters $\sin^2\theta_W$ and m_t^2 , appearing in the LO effective Hamiltonian, amounts to roughly 4% and 7%, respectively, leading to a

TABLE I. Input parameters used in our numerical analysis.

Parameter	Value	Reference
M_Z	91.1876(21) GeV	[21]
M_H	155(40) GeV	
M_t^{TEV}	173.3(1.1) GeV	[22]
$m_c(m_c)$	1.279(13) GeV	[23]
$\hat{s}_{\text{ND}}^2(M_Z)$	0.2315(13)	[21]
κ_+	$0.5173(25) \times 10^{-10}$	[24]
κ_L	$2.231(13) \times 10^{-10}$	[24]
$ \epsilon_K $	$2.228(11) \times 10^{-3}$	[21]
$\alpha_s(M_Z)$	0.1184(7)	[21]
$\hat{\alpha}^{-1}(M_Z)$	127.925(16)	[21]
G_F	$1.166367(5) \times 10^{-5} \text{ GeV}^{-2}$	[21]
λ	0.2255(7)	[25]
$ V_{cb} $	$4.06(13) \times 10^{-2}$	[21]
$\bar{\rho}$	$0.141_{-0.017}^{+0.029}$	[26]
$\bar{\eta}$	0.343(16)	[26]

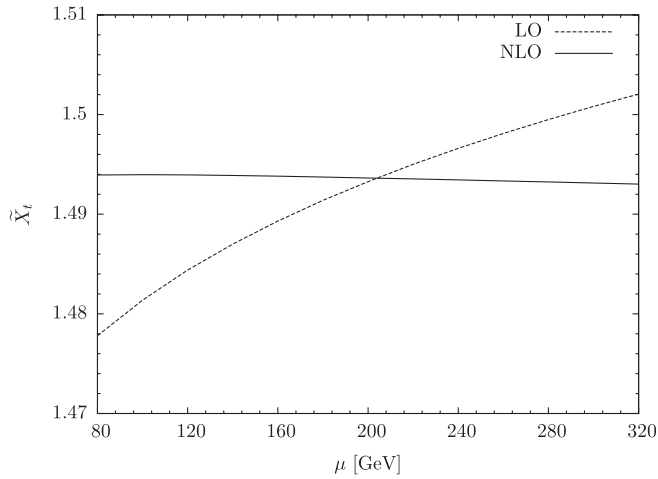


FIG. 3. \tilde{X}_t (see text) as a function of μ , for $M_H = 155$ GeV. The LO result is represented by the dashed line, the solid line includes the full two-loop electroweak corrections, which cancel the μ_t dependence of the LO result almost completely.

large dependence of the branching ratios on the renormalization scheme, if the two-loop electroweak corrections are not included. In turn, we will see that the inclusion of $X_t^{(EW)}$ cancels this ambiguity almost completely. To get a quantitative estimate, we evaluate the function X_t numerically in the three renormalization schemes described in Sec. II.

In Fig. 4 we show \tilde{X}_t in dependence on the Higgs-boson mass M_H , where all couplings are defined in the $\overline{\text{MS}}$ scheme and all masses in the on-shell scheme. In this scheme the NLO electroweak corrections are tiny, of the order of 1 per mil, even for very large Higgs masses.

In Fig. 5 we compare the results in two other schemes. In the left panel we show \tilde{X}_t , where all parameters are defined

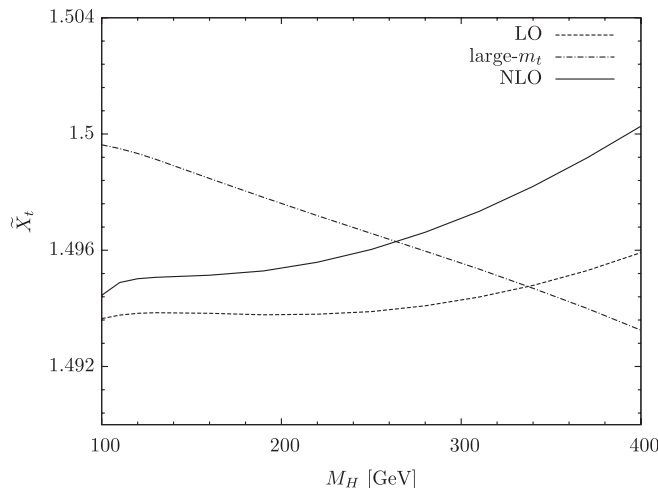


FIG. 4. \tilde{X}_t as a function of M_H . The LO result is represented by the dashed line, the solid line shows the result including the full two-loop electroweak corrections. The NLO corrections in the limit of large top-quark mass are represented by the dashed-dotted line.

in the $\overline{\text{MS}}$ scheme. In the right panel, all parameters are defined in the on-shell scheme, apart from α , which is defined in the $\overline{\text{MS}}$ scheme. As expected, we observe that for the on-shell definition of $\sin^2\theta_W$ (right panel) the related ambiguity is cancelled by a sizeable ($\approx 4\%$) two-loop correction, whereas for the full $\overline{\text{MS}}$ definition (left panel) the electroweak corrections amount to 1%.

We thus conclude that the on-shell definition of the masses together with the $\overline{\text{MS}}$ definition of $\sin^2\theta_W$ is the best choice of the renormalization scheme. We can read off the maximal difference of the three renormalization schemes from the two NLO curves in Fig. 5, right panel – it amounts to 0.27%. For our numerics below, we will take the average of the two curves and assign an error of $\pm 0.134\%$ to X_t , as resulting from the remaining uncertainty of the electroweak correction. In total, using the central values from Table I, we have

$$X_t = 1.469 \pm 0.017 \pm 0.002, \quad (4.2)$$

where the first error quantifies the remaining scale uncertainty of the QCD corrections, and the second error corresponds to the uncertainty of the electroweak corrections. Here and below, we determine the QCD error on X_t by varying the scale μ_c between 80 GeV and 320 GeV. Accordingly, our central value of X_t is the average of $\max_{\mu} X_t(\mu)$ and $\min_{\mu} X_t(\mu)$, where $\mu \in [60 \text{ GeV}, 320 \text{ GeV}]$.

Next, let us comment on the validity of the large- m_t expansion of the full result, which can be gleaned from Fig. 5: It is now evident that it is always a bad approximation to the full result, as has actually been expected before [9,29].

For convenience we provide an approximate, yet very accurate formula for the NLO electroweak correction factor $r_X = 1 + X_t^{(EW)}/X_t^{(0)}$:

$$r_X = 1 - A + B \cdot C^{(M_t/165 \text{ GeV})} - D \left(\frac{M_t}{165 \text{ GeV}} \right), \quad (4.3)$$

where

$$A = 1.11508, \quad B = 1.12316, \quad C = 1.15338, \\ D = 0.179454. \quad (4.4)$$

It approximates the full result within the limits $160 \text{ GeV} \leq M_t \leq 170 \text{ GeV}$ to an accuracy of better than $\pm 0.05\%$.

Finally, we update the theoretical prediction of the branching ratios, including the effect of the full two-loop electroweak corrections. After summation over the three neutrino flavors the resulting branching ratio for $K^+ \rightarrow \pi^+ \nu \bar{\nu}$ can be written as² [1,2,30]

²We have omitted a term which arises from the implicit sum over lepton flavors in P_c because it amounts to only 0.2% of the branching ratio.

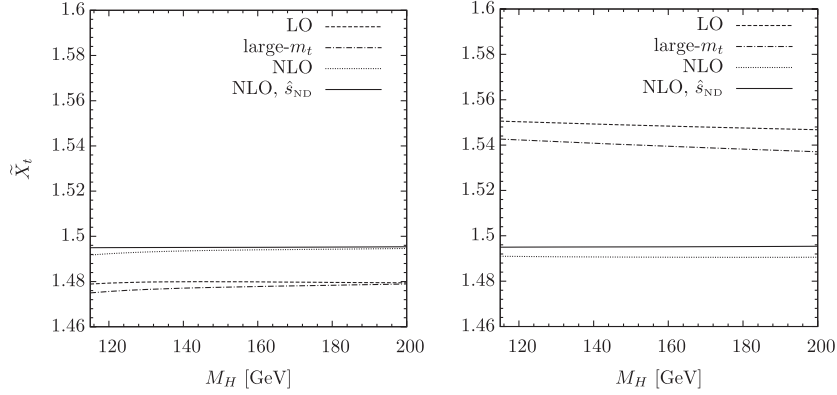


FIG. 5. \tilde{X}_t as a function of M_H , in two different renormalization schemes. The dashed lines show the LO results, the dashed-dotted lines the LO results including the electroweak corrections in the large- m_t limit. The full two-loop results are represented by the dotted lines. The left panel shows the results where all parameters are defined in the $\overline{\text{MS}}$ scheme. By contrast, in the right panel, all parameters apart from α are defined in the on-shell scheme. For comparison, we also plot in both panels the NLO result, where all masses are defined on-shell and all couplings in the $\overline{\text{MS}}$ scheme. It is represented by the solid lines.

$$\begin{aligned} \text{Br}(K^+ \rightarrow \pi^+ \nu \bar{\nu}(\gamma)) & \\ &= \kappa_+ (1 + \Delta_{\text{EM}}) \left[\left(\frac{\text{Im}\lambda_t}{\lambda^5} X_t \right)^2 \right. \\ & \quad \left. + \left(\frac{\text{Re}\lambda_c}{\lambda} (P_c + \delta P_{c,u}) + \frac{\text{Re}\lambda_t}{\lambda^5} X_t \right)^2 \right]. \end{aligned} \quad (4.5)$$

The parameter

$$P_c(X) = \frac{1}{\lambda^4} \left(\frac{2}{3} X^e + \frac{1}{3} X^\tau \right) \quad (4.6)$$

describes the short-distance contribution of the charm quark, where $\lambda = |V_{us}|$, and has been calculated including electroweak corrections, in Ref. [6]. The charm-quark contribution of dimension-eight operators at the charm-quark scale μ_c [31] combined with long-distance contributions were calculated in Ref. [30] to be

$$\delta P_{c,u} = 0.04 \pm 0.02. \quad (4.7)$$

The hadronic matrix element of the low-energy effective Hamiltonian can be extracted from the well-measured K_{l3} decays, including isospin breaking and long-distance QED radiative corrections [24,32,33]. The long-distance contributions are contained in the parameters κ_+ , including NLO and partially next-to-next-to-leading-order corrections in chiral perturbation theory. Δ_{EM} denotes the long-distance QED corrections [24].

Including the two-loop electroweak corrections to X_t , we find for the branching ratio of the charged mode

$$\text{Br}(K^+ \rightarrow \pi^+ \nu \bar{\nu}) = (7.81_{-0.71}^{+0.80} \pm 0.29) \times 10^{-11}, \quad (4.8)$$

The first error is related to the uncertainties in the input parameters. The main contributions are (V_{cb} :56%, $\bar{\rho}$:21%, m_c :8%, m_t :6%, $\bar{\eta}$:4%, α_s :3%, $\sin^2\theta_W$:1%). The second error quantifies the remaining theoretical uncertainty. In detail, the contributions are ($\delta P_{c,u}$:46%, $X_t(\text{QCD})$:24%, P_c :20%, κ_+ :7%, $X_t(\text{EW})$:3%), respectively.

The branching ratio of the CP -violating neutral mode involves the top-quark contribution only and can be written as

$$\text{Br}(K_L \rightarrow \pi^0 \nu \bar{\nu}) = \kappa_L \left(\frac{\text{Im}\lambda_t}{\lambda^5} X_t \right)^2. \quad (4.9)$$

Again, the hadronic matrix element can be extracted from the K_{l3} decays and is now parametrized by κ_L [24]. There are no more long-distance contributions, which makes this decay channel exceptionally clean.

Whereas the CP -conserving contribution to the branching ratio is completely negligible compared to the direct CP -violating contribution within the standard model [34], the indirect CP -violating contribution is of the order of 1% and should be included at the current level of accuracy. This can be achieved by multiplying the branching ratio with the factor [35]

$$1 - \sqrt{2} |\epsilon_K| \frac{1 + P_c(X)/(A^2 X_t) - \rho}{\eta}, \quad (4.10)$$

where $A = V_{cb}/\lambda^2$, and ϵ_K describes indirect CP violation in the neutral Kaon system. Taking this factor into account, and including again the full two-loop electroweak corrections, we find

$$\text{Br}(K_L \rightarrow \pi^0 \nu \bar{\nu}) = (2.43_{-0.37}^{+0.40} \pm 0.06) \times 10^{-11}. \quad (4.11)$$

The first error is again related to the uncertainties in the input parameters. Here main contributions are (V_{cb} :54%, $\bar{\eta}$:39%, m_t :6%). The contributions to the second, theoretical uncertainty are ($X_t(\text{QCD})$:73%, κ_L :18%, $X_t(\text{EW})$:8%, $\delta P_{c,u}$:1%), respectively. All errors have been added in quadrature.

V. CONCLUSIONS

In this paper, we have calculated the complete two-loop electroweak matching corrections to X_t , the top-quark contribution to the rare decays $K_L \rightarrow \pi^0 \nu \bar{\nu}$, $K^+ \rightarrow \pi^+ \nu \bar{\nu}$, and $B \rightarrow X_{d,s} \nu \bar{\nu}$. This is, in particular, important for rare kaon decays: future proposals aim at an experimental accuracy of 3% for the branching ratios, while the leading-order electroweak scheme ambiguity is of similar size. Our calculation reduces the scheme ambiguity in X_t from $\pm 2\%$ to $\pm 0.134\%$. The resulting theory uncertainty in the branching ratios is rendered from dominant to negligible.

The absolute corrections are small in a renormalization scheme where on-shell masses and $\overline{\text{MS}}$ coupling constants are used for the electroweak sector. In addition, we analyze the convergence in the $\overline{\text{MS}}$ scheme and the on-shell scheme to estimate the remaining perturbative uncertainty.

Our analytic results are summarized by an approximate, but very accurate formula. We also give the leading term in a small $\sin\theta_W$ expansion. The full expression can be obtained upon request from the authors.

ACKNOWLEDGMENTS

We would like to thank G. Buchalla, A. Buras, and P. Gambino for useful discussions and comments.

APPENDIX A: $\sin\theta_W$ EXPANSION

The explicit expression of the full two-loop electroweak correction $X_t^{(EW)}$ is too long to be given explicitly here. The result significantly simplifies if we expand in the small parameter $\sin\theta_W$ —see Fig. 6 for the validity of the expansion. In the $\overline{\text{MS}}$ scheme, after normalizing the effective Hamiltonian to G_F , we find

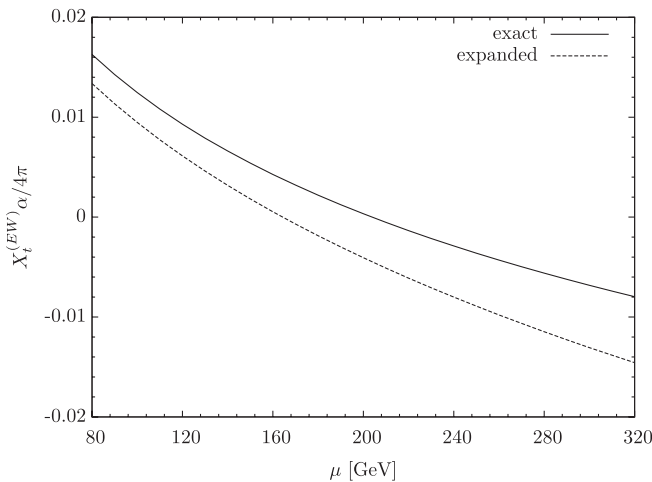


FIG. 6. The $\sin\theta_W$ expansion of $X_t^{(EW)} \alpha / 4\pi$ in the $\overline{\text{MS}}$ scheme as a function of the renormalization scale μ . The solid line shows the full result, while the dashed line corresponds to the leading term of the expansion.

$$X_t^{(EW)}(x_t, a, \hat{s}_{\text{ND}}, \mu) = \frac{1}{128\hat{s}_{\text{ND}}^2} \left(\sum_{i=1}^{17} c_i A_i + \mathcal{O}(\hat{s}_{\text{ND}}) \right), \quad (\text{A1})$$

where $a = (M_H/m_t^{\overline{\text{MS}}})^2$,

$$\begin{aligned} c_1 &= \frac{1}{3a(x_t - 1)^2 x_t}, & c_2 &= \frac{1}{(x_t - 1)^3 (ax_t - 1)} \varphi_1\left(\frac{1}{4}\right), \\ c_3 &= \frac{1}{2(x_t - 1)^3 (ax_t - 1)} \varphi_1\left(\frac{a}{4}\right), \\ c_4 &= \frac{1}{2(x_t - 1)^3 (ax_t - 1)} \varphi_1\left(\frac{1}{4x_t}\right), \\ c_5 &= \frac{1}{2(x_t - 1)^3 (ax_t - 1)} \varphi_1\left(\frac{x_t}{4}\right), \\ c_6 &= \frac{1}{(x_t - 1)^3 (ax_t - 1)} \varphi_1\left(\frac{ax_t}{4}\right), \\ c_7 &= \frac{1}{2a^2 x_t^2 (x_t - 1)^3 (ax_t - 1)} \varphi_2\left(\frac{1}{ax_t}, \frac{1}{a}\right), \\ c_8 &= \frac{1}{ax_t - 1} \log^2(a), \end{aligned}$$

$$c_9 = \frac{1}{3(x_t - 1)^3 (ax_t - 1)} \log(x_t),$$

$$c_{10} = \frac{1}{2a(x_t - 1)^4 x_t (ax_t - 1)} \log^2(x_t),$$

$$c_{11} = \frac{1}{(x_t - 1)^2} \log\left(\frac{\mu^2}{M_W^2}\right),$$

$$c_{12} = \frac{1}{(x_t - 1)^3} \log(x_t) \log\left(\frac{\mu^2}{M_W^2}\right),$$

$$c_{13} = \frac{1}{(x_t - 1)^2 (ax_t - 1)} \log(a),$$

$$c_{14} = \frac{1}{2a(x_t - 1)^3 (ax_t - 1)} \log(x_t) \log(a),$$

$$c_{15} = \frac{1}{(x_t - 1)^2} \text{Li}_2(1 - a), \quad c_{16} = \frac{1}{ax_t} \text{Li}_2(1 - x_t),$$

$$c_{17} = \frac{1}{a(x_t - 1)^2 x_t} \text{Li}_2(1 - ax_t),$$

and

$$\begin{aligned} A_1 &= +(16 - 48a)\pi^2 + (288a - (32 - 88a)\pi^2)x_t \\ &+ (2003a + 4(4 - 6a - a^2)\pi^2)x_t^2 + (9a(93 + 28a) \\ &- 4a(3 - 2a + 8a^2)\pi^2)x_t^3 + (3a(172 - 49a - 32a^2) \\ &+ 4a(20 - a + 16a^2)\pi^2)x_t^4 - (3a(168 + 11a - 24a^2) \\ &+ 4a(45 + 8a^2)\pi^2)x_t^5 + 96a\pi^2 x_t^6, \end{aligned}$$

$$A_2 = -768x_t - (525 - 867a)x_t^2 + (303 + 318a)x_t^3 - 195ax_t^4,$$

$$A_3 = -8(95 - 67a + 11a^2)x_t^2 + 2(662 - 78a - 177a^2 + 40a^3)x_t^3 - (608 + 476a - 595a^2 + 114a^3)x_t^4 \\ + (44 + 188a - 321a^2 + 103a^3 - 8a^4)x_t^5 - a(28 - 72a + 33a^2 - 4a^3)x_t^6,$$

$$A_4 = +48 - 10(57 + 4a)x_t + 51(29 + 10a)x_t^2 - (841 + 1265a)x_t^3 + (308 + 347a)x_t^4 - (28 - 40a)x_t^5 + 12ax_t^6,$$

$$A_5 = +768 + (816 - 768a)x_t + (1240 - 1232a)x_t^2 - 4(415 + 2a)x_t^3 + (311 + 722a)x_t^4 \\ + (145 - 267a)x_t^5 - (36 + 51a)x_t^6 + 20ax_t^7,$$

$$A_6 = +328x_t - (536 + 900a)x_t^2 + (208 + 1584a + 670a^2)x_t^3 - a(668 + 1161a + 225a^2)x_t^4 \\ + a^2(479 + 362a + 28a^2)x_t^5 - a^3(143 + 42a)x_t^6 + 16a^4x_t^7,$$

$$A_7 = +32 - 4(44 - 9a)x_t + (384 - 322a - 400a^2)x_t^2 - (400 - 869a - 1126a^2 - 696a^3)x_t^3 + 2(80 - 488a - 517a^2 \\ - 631a^3 - 264a^4)x_t^4 + (48 + 394a + 269a^2 + 190a^3 + 882a^4 + 196a^5)x_t^5 - (64 - 58a - 89a^2 - 95a^3 + 34a^4 \\ + 296a^5 + 32a^6)x_t^6 + (16 - 59a - 79a^2 + 256a^3 - 239a^4 + 57a^5 + 48a^6)x_t^7 + (1 - a)^3a^2(29 + 16a)x_t^8,$$

$$A_8 = +28a^2x_t^2 - 32a^3x_t^3,$$

$$A_9 = -288 + 36(1 + 8a)x_t + 6(647 + 87a)x_t^2 + 5(55 - 927a - 132a^2)x_t^3 - (1233 + 98a - 879a^2 - 192a^3)x_t^4 \\ + (360 + 1371a - 315a^2 - 264a^3)x_t^5 - 24a(17 - 4a^2)x_t^6,$$

$$A_{10} = +32 + 4(-44 + 29a)x_t - 12(-32 + 77a + 31a^2)x_t^2 + 2(-200 + 837a + 767a^2 + 182a^3)x_t^3 \\ - 2(-80 + 625a + 905a^2 + 520a^3 + 82a^4)x_t^4 + (48 + 1079a + 590a^2 + 1002a^3 + 462a^4 + 32a^5)x_t^5 \\ + (-64 - 1160a - 501a^2 - 364a^3 - 486a^4 - 72a^5)x_t^6 + (16 + 729a + 1038a^2 + 38a^3 + 238a^4 + 52a^5)x_t^7 \\ - a(192 + 743a + 50a^3 + 12a^4)x_t^8 + 192a^2x_t^9,$$

$$A_{11} = +16x_t + 324x_t^2 - 36x_t^4, \quad A_{12} = +216x_t - 672x_t^2 + 152x_t^3,$$

$$A_{13} = -16x_t + (16 - 42a)x_t^2 + (16 + 21a + 60a^2)x_t^3 - (16 - 21a + 45a^2 + 32a^3)x_t^4 - a^2(7 - 24a)x_t^5,$$

$$A_{14} = -32 + (144 - 68a)x_t + (-240 + 334a + 332a^2)x_t^2 + (160 - 551a - 660a^2 - 364a^3)x_t^3 \\ + a(329 + 451a + 650a^2 + 164a^3)x_t^4 + (-48 - a - 59a^2 - 523a^3 - 316a^4 - 32a^5)x_t^5 \\ + (16 - 43a - 93a^2 + 255a^3 + 287a^4 + 32a^5)x_t^6 - a^2(-29 + 42a + 103a^2 + 8a^3)x_t^7,$$

$$A_{15} = -144(1 - a)^2x_t^2 + 144(1 - a)^2x_t^3 - 36(1 - a)^2x_t^4,$$

$$A_{16} = -32 + 96a + (48 - 32a)x_t - 176ax_t^2 - (16 - 74a)x_t^3 + 212ax_t^4,$$

$$A_{17} = -32 + (64 - 100a)x_t - 8(4 - 34a - 29a^2)x_t^2 - 4a(34 + 170a + 33a^2)x_t^3 \\ + 8a^2(47 + 51a + 4a^2)x_t^4 - 16a^3(15 + 4a)x_t^5 + 32a^4x_t^6.$$

Here we use

$$\text{Li}_2(\xi) = - \int_0^1 \frac{\log(1 - \xi t)}{t} dt,$$

and the two-loop functions φ_1 and φ_2 are given by [17]

$$\varphi_1(z) = \begin{cases} 4\sqrt{\frac{z}{1-z}} \text{Cl}_2(2 \arcsin(\sqrt{z})), & 0 \leq z < 1, \\ \frac{1}{\lambda_z} \left(2\ln^2 \frac{1-\lambda_z}{2} - 4\text{Li}_2 \frac{1-\lambda_z}{2} - \ln^2(4z) + \frac{1}{3}\pi^2 \right), & z > 1, \end{cases} \quad (\text{A2})$$

and

$$\varphi_2(x, y) = \begin{cases} \frac{1}{\lambda} \left\{ \frac{\pi^2}{3} + 2\ln\left(\frac{1}{2}(1+x-y-\lambda)\right) \ln\left(\frac{1}{2}(1-x+y-\lambda)\right) - \ln x \ln y - 2\text{Li}_2\left(\frac{1}{2}(1+x-y-\lambda)\right) \right. \\ \left. - 2\text{Li}_2\left(\frac{1}{2}(1-x+y-\lambda)\right) \right\}, & \lambda^2 \geq 0, \sqrt{x} + \sqrt{y} \leq 1, \\ \frac{2}{\sqrt{-\lambda^2}} \left\{ \text{Cl}_2\left(2 \arccos\left(\frac{-1+x+y}{2\sqrt{xy}}\right)\right) + \text{Cl}_2\left(2 \arccos\left(\frac{1+x-y}{2\sqrt{x}}\right)\right) + \text{Cl}_2\left(2 \arccos\left(\frac{1-x+y}{2\sqrt{y}}\right)\right) \right\}, & \lambda^2 \leq 0, \sqrt{x} + \sqrt{y} \geq 1. \end{cases} \quad (\text{A3})$$

Here $\lambda_z = \sqrt{1-1/z}$ and $\lambda = \sqrt{(1-x-y)^2 - 4xy}$. The Clausen function is defined by $\text{Cl}_2(z) = -\int_0^\theta d\theta \ln|2 \sin(\theta/2)|$.

APPENDIX B: THE LARGE- m_t EXPANSION

The two-loop electroweak corrections to the bbZ vertex, denoted by $\tau_b^{(2)}$, have been calculated in the limit of a large top-quark mass by Barbieri *et al.* in [36,37] and were confirmed by Fleischer, Tarasov, and Jegerlehner [38], who found a particularly simple analytic form of the results. Buchalla and Buras have extracted from this result the corrections to the sdZ vertex, which they used for their analysis of the $K \rightarrow \pi\nu\bar{\nu}$ decays in [9]. We will now take the limit $m_t \rightarrow \infty$ in our complete result for the $sd\nu\nu$ transition and compare it with the result in [38].

Several important points should be mentioned here: As observed in [9], only Z penguin diagrams contribute to the $sd\nu\nu$ transition in the large- m_t limit. The results in [38] have been obtained in the so-called ‘‘gaugeless limit,’’ where, in particular, the W boson field does not appear. Accordingly, the parameter corresponding to our x_t is defined in [38] by $x_t \equiv \sqrt{2}G_\mu m_t^2/(16\pi^2)$ and will be denoted by \tilde{x}_t in our paper. As a consequence, the result for $\tau_b^{(2)}$ is normalized to G_F^2 in [38]. On the other hand, we performed a full standard model calculation and afterwards took the limit $m_t \rightarrow \infty$.

Thus we now take the large- m_t expansion of our result, factor out G_F^2 , and perform a finite renormalization of the top-quark mass in our LO result, by replacing $m_t^{\overline{\text{MS}}} = M_t + \delta M_t$, in order to transform into the on-shell scheme. Here δM_t is given in the large- m_t limit by

$$\frac{\delta M_t}{M_t} = \frac{e^2}{16\pi^2 s_W^2} x_t \left(\frac{3}{a} + 1 - \frac{1}{2}a - \frac{1}{16}(4a^{1/2} - a^{3/2})g(a) + \frac{1}{16}a^2 \log a \right), \quad (\text{B1})$$

and

$$g(a) = 2\sqrt{a-4} \left[\text{arctanh}\left(\frac{2-a}{\sqrt{(a-4)a}}\right) + \text{arctanh}\left(\sqrt{\frac{a}{a-4}}\right) \right]. \quad (\text{B2})$$

In this way we reproduce the result in [38]:

$$\begin{aligned} \tau_b^{(2), \text{on-shell}} &= 9 - \frac{13}{4}a - 2a^2 - \left(\frac{1}{24} + \frac{7}{12}a^2 - \frac{1}{2}a^3\right)\pi^2 \\ &\quad - \left(\frac{19}{4}a + \frac{3}{2}a^2\right) \ln a - \left(\frac{7}{4}a^2 - \frac{3}{2}a^3\right) \ln^2 a \\ &\quad - \left(\frac{7}{4} - \frac{15}{2}a + \frac{39}{4}a^2 - 4a^3\right) \text{Li}_2(1-a) \\ &\quad - (2 - \frac{a}{2})\sqrt{a}g(a) - \frac{1}{2}\left(7 - 18a + \frac{33}{4}a^2 - a^3\right)\varphi_1\left(\frac{a}{4}\right). \end{aligned} \quad (\text{B3})$$

It corresponds to the effective Hamiltonian in the limit of large top-quark mass

$$\mathcal{H}_{\text{eff}} = \frac{4G_F}{\sqrt{2}} \frac{\alpha}{2\pi \sin^2 \theta_W} \lambda_t \left(\frac{x_t}{8} + \frac{\alpha}{4\pi 32 \sin^2 \theta_W} (3 + \tau_b^{(2)}) \right) Q_\nu. \quad (\text{B4})$$

Our result in the $\overline{\text{MS}}$ scheme is given by

$$\begin{aligned} \tau_b^{(2), \overline{\text{MS}}} &= -2 - \frac{11}{4}a - 2a^2 - \left(\frac{1}{24} + \frac{7}{12}a^2 - \frac{a^3}{2}\right)\pi^2 \\ &\quad - \left(\frac{7}{4}a + 2a^2\right) \ln a - \left(\frac{7}{4}a^2 - \frac{3}{2}a^3\right) \ln^2 a \\ &\quad - \left(\frac{7}{4} - \frac{15}{2}a + \frac{39}{4}a^2 - 4a^3\right) \text{Li}_2(1-a) \\ &\quad - \frac{1}{2}\left(7 - 18a + \frac{33}{4}a^2 - a^3\right)\varphi_1\left(\frac{a}{4}\right) \end{aligned} \quad (\text{B5})$$

for $\mu_t = M_t$. It is normalized to G_F and thus independent of the tadpole contribution.

- [1] G. Buchalla and A.J. Buras, *Nucl. Phys.* **B412**, 106 (1994).
- [2] G. Buchalla and A.J. Buras, *Nucl. Phys.* **B548**, 309 (1999).
- [3] M. Gorbahn and U. Haisch, *Nucl. Phys.* **B713**, 291 (2005).
- [4] A.J. Buras, M. Gorbahn, U. Haisch, and U. Nierste, *Phys. Rev. Lett.* **95**, 261805 (2005).
- [5] A.J. Buras, M. Gorbahn, U. Haisch, and U. Nierste, *J. High Energy Phys.* **11** (2006) 002.
- [6] J. Brod and M. Gorbahn, *Phys. Rev. D* **78**, 034006 (2008).
- [7] G. Buchalla and A.J. Buras, *Nucl. Phys.* **B398**, 285 (1993).
- [8] M. Misiak and J. Urban, *Phys. Lett. B* **451**, 161 (1999).
- [9] G. Buchalla and A.J. Buras, *Phys. Rev. D* **57**, 216 (1998).
- [10] T. Inami and C. S. Lim, *Prog. Theor. Phys.* **65**, 297 (1981); **65**, 1772(E) (1981).
- [11] W.J. Marciano and A. Sirlin, *Phys. Rev. Lett.* **61**, 1815 (1988).
- [12] T. van Ritbergen and R. G. Stuart, *Nucl. Phys.* **B564**, 343 (2000).
- [13] F. Jegerlehner, M. Y. Kalmykov, and O. Veretin, *Nucl. Phys.* **B641**, 285 (2002).
- [14] F. Jegerlehner, M. Y. Kalmykov, and O. Veretin, *Nucl. Phys.* **B658**, 49 (2003).
- [15] G. Degrassi, P. Gambino, and A. Sirlin, *Phys. Lett. B* **394**, 188 (1997).
- [16] C. Bobeth, M. Misiak, and J. Urban, *Nucl. Phys.* **B574**, 291 (2000).
- [17] A.I. Davydychev and J.B. Tausk, *Nucl. Phys.* **B397**, 123 (1993).
- [18] T. Hahn, *Comput. Phys. Commun.* **140**, 418 (2001).
- [19] J. A. M. Vermaseren, [arXiv:math-ph/0010025](https://arxiv.org/abs/math-ph/0010025).
- [20] T. L. Trueman, *Z. Phys. C* **69**, 525 (1996).
- [21] K. Nakamura, *J. Phys. G* **37**, 075021 (2010).
- [22] Tevatron Electroweak Working Group, [arXiv:1007.3178](https://arxiv.org/abs/1007.3178).
- [23] K. G. Chetyrkin *et al.*, *Phys. Rev. D* **80**, 074010 (2009).
- [24] F. Mescia and C. Smith, *Phys. Rev. D* **76**, 034017 (2007).
- [25] M. Antonelli *et al.*, [arXiv:0801.1817](https://arxiv.org/abs/0801.1817).
- [26] J. Charles *et al.*, *Eur. Phys. J. C* **41**, 1 (2005).
- [27] M. Awramik, M. Czakon, A. Freitas, and G. Weiglein, *Phys. Rev. D* **69**, 053006 (2004).
- [28] K. G. Chetyrkin, J. H. Kuhn, and M. Steinhauser, *Comput. Phys. Commun.* **133**, 43 (2000).
- [29] P. Gambino, A. Kwiatkowski, and N. Pott, *Nucl. Phys.* **B544**, 532 (1999).
- [30] G. Isidori, F. Mescia, and C. Smith, *Nucl. Phys.* **B718**, 319 (2005).
- [31] A. F. Falk, A. Lewandowski, and A. A. Petrov, *Phys. Lett. B* **505**, 107 (2001).
- [32] W. J. Marciano and Z. Parsa, *Phys. Rev. D* **53**, R1 (1996).
- [33] J. Bijnens and K. Ghorbani, [arXiv:0711.0148](https://arxiv.org/abs/0711.0148).
- [34] G. Buchalla and G. Isidori, *Phys. Lett. B* **440**, 170 (1998).
- [35] G. Buchalla and A.J. Buras, *Phys. Rev. D* **54**, 6782 (1996).
- [36] R. Barbieri, M. Beccaria, P. Ciafaloni, G. Curci, and A. Vicere, *Nucl. Phys.* **B409**, 105 (1993).
- [37] R. Barbieri, M. Beccaria, P. Ciafaloni, G. Curci, and A. Vicere, *Phys. Lett. B* **288**, 95 (1992).
- [38] J. Fleischer, O. V. Tarasov, and F. Jegerlehner, *Phys. Rev. D* **51**, 3820 (1995).